Free Radical Research, September 2010; 44(9): 1072–1081

informa
healthcare

Novel polyhydroxylated fullerene suppresses intracellular oxidative stress together with repression of intracellular lipid accumulation during the differentiation of OP9 preadipocytes into adipocytes

YASUKAZU SAITOH[1], LI XIAO[1], HIROMI MIZUNO[1], SHINYA KATO[1], HISAE AOSHIMA[2], HIKARU TAIRA[2], KEN KOKUBO[3] & NOBUHIKO MIWA[1]

[1]*Laboratory of Cell-Death Control BioTechnology, Faculty of Life and Environmental Sciences, Prefectural University of Hiroshima, 562 Nanatsuka, Shobara, Hiroshima 727-0023, Japan,* [2]*Vitamin C60 BioResearch Corporation, Tatsunuma Tatemono Bldg., 9F, 1-3-19 Yaesu Chuo-ku, Tokyo 103-0028, Japan, and* [3]*Division of Applied Chemistry, Graduate School of Engineering, Osaka University, 2-1 Yamadaoka, Suita, Osaka 565-0871, Japan*

(Received date: 16 March 2010; In revised form date: 27 May 2010)

Abstract

Along with differentiation of mouse stromal preadipocytes OP9 into adipocytes, intracellular ROS, especially superoxide anion radicals detected by NBT reduction assay, were found to appreciably increase, mainly in cytoplasmic area, parallelling with increases in intracellular lipid-droplet accumulation, whereas undifferentiated OP9 cells kept lower levels of ROS and lipid-droplets. β-Carotene bleaching assay showed that super-highly hydroxylated fullerene (SHH-F; C_{60} $(OH)_{44}$) exerted higher anti-oxidant ability than highly hydroxylated fullerene (HH-F; C_{60} $(OH)_{32-34}$) or lowly hydroxylated fullerene (LH-F; C_{60} $(OH)_{6-12}$). Differentiation-dependent lipid-droplet accumulation was suppressed by SHH-F or HH-F more efficiently than LH-F. Furthermore, SHH-F significantly repressed intracellular ROS generation accompanied by adipocyte differentiation. Thus, lipid-droplet accumulation was shown to positively correlate with ROS upon the differentiation of OP9 preadipocytes into adipocytes and SHH-F significantly suppressed intracellular ROS together with repression of intracellular lipid accumulation.

Keywords: *Fullerenol, adipocytes, lipid accumulation, reactive oxygen species, antioxidative activity, differentiation*

Introduction

Polyhydroxylated fullerenes (fullerenols; $C_{60}(OH)_n$) are water-soluble and are known to possess a particular significance as free radical scavengers or antioxidants in biological systems [1–11]. It has been also reported that fullerenols exerted inhibitory effects against diverse cell injuries such as brain cell damage by peroxide [3], damage of the bronchial asthma model [12], reactive oxygen species (ROS)-mediated neuronal death [10,13], oxidative stress in both the RAW 264.7 macrophage cell line and ischemia-reperfused rat lungs [14], doxorubicin toxicity in human breast cancer cell lines [15], proliferation of vascular smooth muscle cell lines [16], neutrophilic lung inflammation in mice [17] and mitochondrial dysfunction in a cellular model of Parkinson's disease [18]. Thus, fullerenols seem to be valuable candidates for prophylactic and/or therapeutic agents against ROS related disease due to their properties as free radical scavengers and antioxidants.

Obesity is a primary causative factor in the development of metabolic syndrome, which is closely implicated in various diseases such as hypertension, insulin resistance, type II diabetes, coronary artery disease and heart failure [19]. Recently, ROS has been suggested to be one of the key factors associated with the development of obesity. It has been demonstrated that ROS production was increased during differentiation into adipocytes and administration with free fatty acid could induce ROS production in 3T3-L1 adipocytes

Correspondence: N. Miwa, Laboratory of Cell-Death Control BioTechnology, Faculty of Life and Environmental Sciences, Prefectural University of Hiroshima, Nanatsuka 562, Shobara, Hiroshima 727-0023, Japan. Tel/Fax: +81 824 74 1754. Email: miwa-nob@pu-hiroshima.ac.jp

ISSN 1071-5762 print/ISSN 1029-2470 online © 2010 Informa UK Ltd.
DOI: 10.3109/10715762.2010.499905

[20]. Furthermore, it has also been described that increased markers of oxidative stress were observed in obese humans [21] and rodents [20,22,23]. Therefore, these findings imply that ROS scavengers are expected to be effective in preventing obesity-associated metabolic syndrome. Differentiation from preadipocytes to adipocytes is a well-known crucial process for development of obesity and obesity is characterized by an increase in the number and size of adipocytes containing considerable lipid droplets at the cell biological level. Preadipocytes cell lines are useful models for investigating the adipogenesis process and the OP9 cell line was recently suggested as a novel model appropriate for studying the basal differentiation step [24].

In the present study, we used the novel polyhydroxylated fullerene (C_{60} $(OH)_{44}\cdot 8H_2O$) and investigated the effects of three types of fullerenols ($C_{60}(OH)_{6-12}$, C_{60} $(OH)_{32-34}\cdot 7H_2O$ and C_{60} $(OH)_{44}\cdot 8H_2O$) on intracellular lipid accumulation and intracellular ROS generation during the differentiation of OP9 preadipocytes into adipocytes. Consequently, C_{60} $(OH)_{44}\cdot 8H_2O$ showed a stronger antioxidative activity than two other fullerenols and markedly suppressed differentiation-dependent increases in intracellular lipid accumulation and ROS generation during differentiation.

Materials and methods

Cell culture and differentiation into adipocytes

OP9 cells, a line of bone marrow-derived mouse stromal cells, were obtained from the American Type Culture Collection (Manassas, VA; catalogue no. CRL-2749). Cells were cultured in MEM-α (Invitrogen Corp., CA) supplemented with 20% heat-inactivated fetal bovine serum (FBS, Biological Industries Ltd., Beit Haemek, Israel), 100 U/ml penicillin and 100 mg/l streptomycin at 37°C in a humidified atmosphere of 95% air and 5% CO_2. Adipocyte differentiation was induced as previously described [24] with minor modification. Briefly, OP9 preadipocytes were seeded at 60,000 cells/cm^2 and grown for 2 days to reach confluency (day 0) and then the cells were treated with culture medium containing 1 μM dexamethasone, 0.5 mM 3-isobutyl-1-methylxanthine (IBMX) with or without fullerenols for 3 days. On day 3, the cells were cultured in culture medium containing 10 μg/ml insulin with or without fullerenols for another 4 days. Typical morphological aspects of OP9 preadipocytes and differentiated adipocytes were represented in Figure 1. Three types of fullerenols were used, lowly hydroxylated fullerene ($C_{60}(OH)_{6-12}$;LH-F) was purchased from Frontier Carbon Corp. (Fukuoka, Japan) and highly hydroxylated fullerene (C_{60} $(OH)_{32-34}\cdot 7H_2O$; HH-F) and super-highly hydroxylated fullerene (C_{60} $(OH)_{44}\cdot 8H_2O$; SHH-F) were synthesized by using a novel method [25] in Osaka University and supplied from Vitamin C60 BioResearch Co. (Tokyo, Japan).

Evaluation of accumulated lipid contents in adipocytes

Differentiation was estimated by microscopic observation and Oil Red O staining [26]. Cells were washed twice with phosphate buffered saline (PBS), fixed in 10% formalin for 30 min and stained for 1 h with Oil Red O solution. Then, they were washed twice with PBS and photographed. In order to determine the amount of lipids, image analysis based on the photographs was conducted by the use of the Image J software (NIH) or extract of the dye from the stained cells was quantified for chromaticity. For quantitative image analysis, stained cells were photographed for three fields per well (nine fields in total under each condition) and the intracellular lipid accumulation level was analysed by Image J software. To extract the dye, 0.25 ml of isopropanol/water (6:4) solution was added to the stained culture-well and the dye was extracted with gentle shaking for 30 min at 25°C. Thereafter, the absorbance at 530 nm was measured with a microplate reader (FLUOstar OPTIMA, BMG Labtech, Offenburg, Germany). Three fullerene derivatives have little absorption at

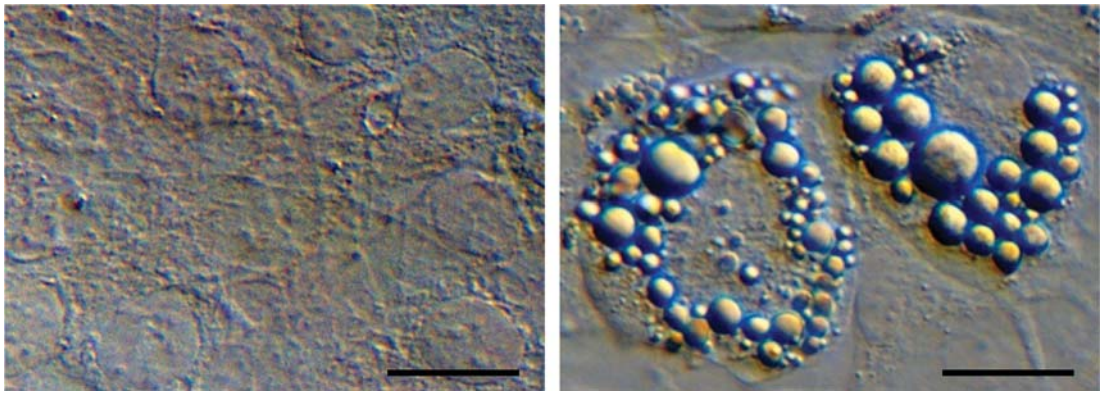

Figure 1. Morphological aspects of OP9 preadipocytes (left) and the differentiated adipocytes (right). OP9 cells were differentiated into adipocytes as described in Materials and methods. The scale bar indicates 25 μm.

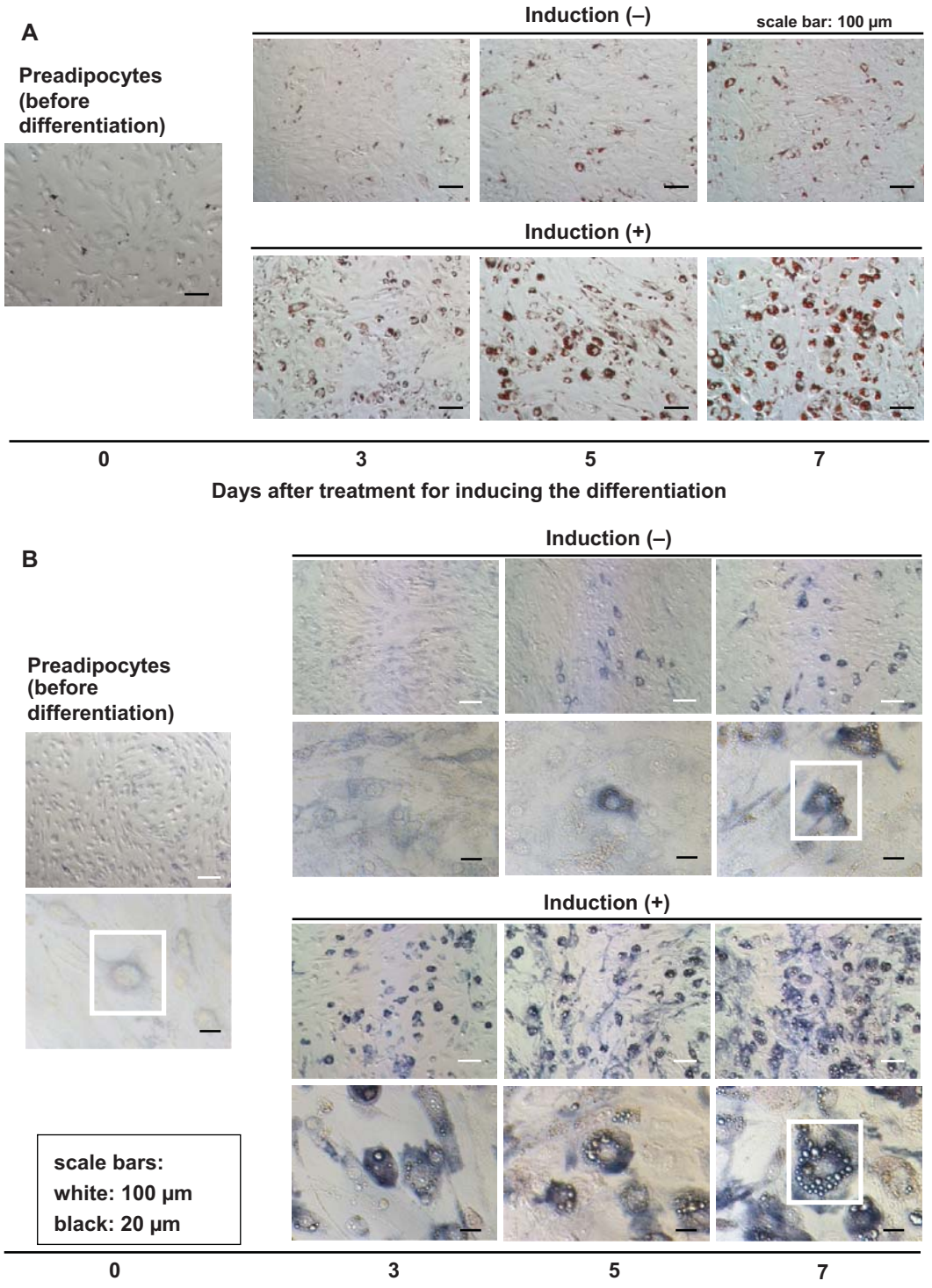

Figure 2. Intracellular ROS production during differentiation of OP9 cells into adipocytes. OP9 cells were differentiated into adipocytes as described in Materials and methods. Intracellular lipid accumulation and ROS production were determined by Oil Red O staining and NBT reduction on the indicated days, respectively. Morphological aspects of Oil Red O-stained (A) and NBT-stained (B) OP9 cells during differentiation into adipocytes were photographed under a microscope. Areas inside the white boxes in (B) were enlarged and represented in (C) and dashed lines show the outline of a cell. The dye or formazan was extracted and the absorbance was measured (D). Correlation of intracellular ROS with lipid accumulation and Pearson's correlation coefficient (r) are shown for each relationship. Each data point was calculated from the average of independent data ($n = 3$) (E). Values are expressed as mean ± SD ($n = 3$). Significantly different from induction (−) at day 0, $^{**}p < 0.01$ (lipid accumulation); $^{\#\#}p < 0.01$ (intracellular ROS).

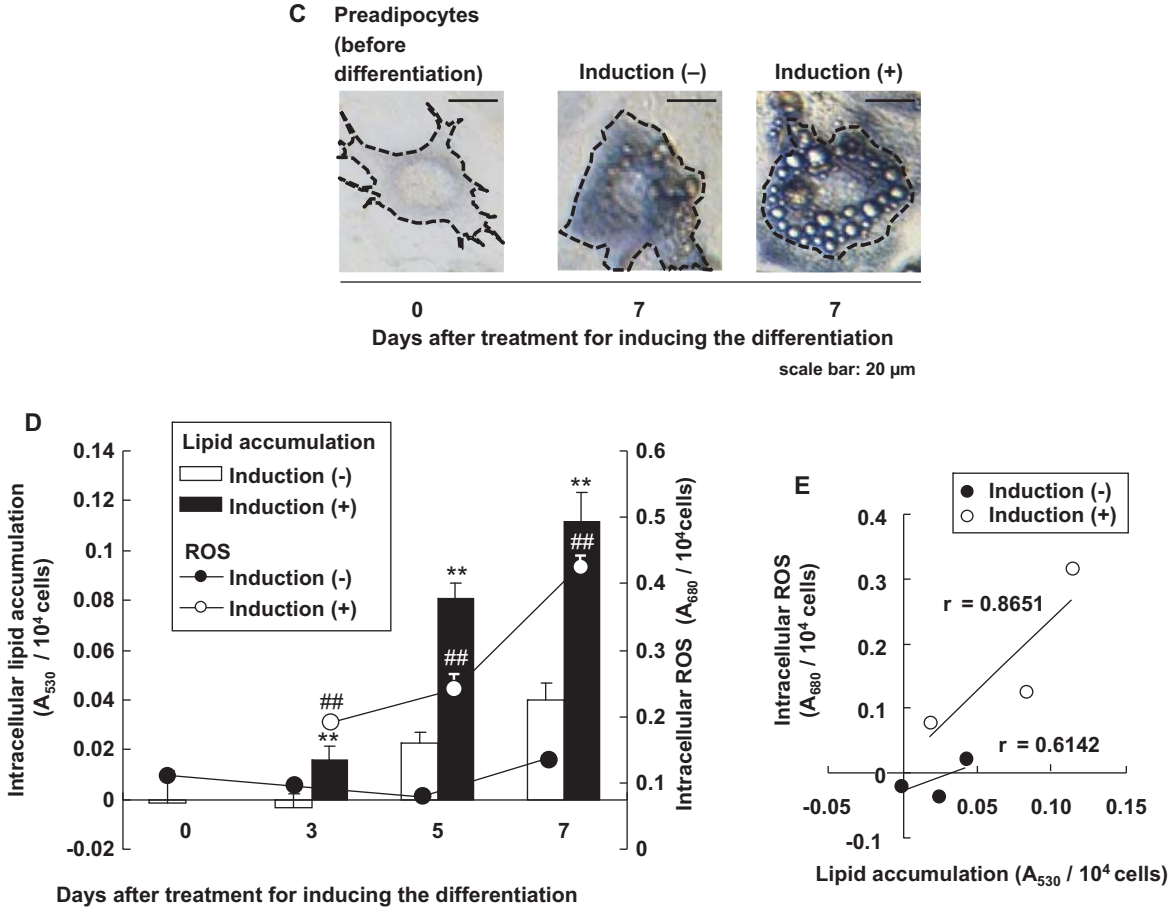

Figure 2. (Continued)

530 nm. On the indicated day, cells were stained with Diff-Quik (Sysmex, Kobe, Japan), photographed for five fields per well (20 fields in total under each condition), counted and calculated for the cell number. Accumulated lipid contents in adipocytes were represented as the amount of intracellular lipid accumulation per 10^4 cells.

Measurement of intracellular generation of superoxide anion radicals

Superoxide generation was detected by nitroblue tetrazolium (NBT) assay [27]. NBT (yellow, water-soluble) (Wako Pure Chemical Industries Ltd., Osaka, Japan) was reduced by superoxide anion radicals to form formazan-NBT (dark-blue, water-insoluble). On the indicated day, cells were rinsed with PR-free MEM and incubated for 90 min in PR-free DMEM containing 0.2% NBT. Cells were rinsed with cold PBS, stained and photographed. Then, the formazan was dissolved in 2 M KOH/DMSO solution for 30 min at 37°C and the absorbance at 680 nm was determined with a microplate reader. Three fullerene derivatives have little absorption at 680 nm.

Assessment of antioxidative activity of hydroxylated fullerene derivatives

Antioxidative activity was assessed by a β-Carotene bleaching method according to the previous reports [7,28]. This is an *in vitro* assay that measures the inhibition of coupled auto-oxidation of linoleic acid and β-Carotene and it can assess an antioxidant activity against lipidperoxyl radicals (LOO•) or lipid radicals (L•) by fading of yellow-orange colour of β-Carotene. Briefly, aliquots of β-Carotene and linoleic acid emulsion were mixed with the solution of hydroxylated fullerene derivatives in disposable cuvettes. The cuvettes were incubated at 50°C in a water-bath for the indicated times. Absorbance at 470 nm of each sample was measured immediately at 0 min and every 20 min up to 180 min. Retention of yellow-orange colour attributed to β-Carotene was expressed as a percentage vs that of the control cells.

Evaluation of cell viability

Cell viability was assessed based on mitochondrial enzymatic conversion of WST-1 [2-(4-iodophenyl)-3-(4-nitrophenyl)-5-(2,4-disulphophenyl)-2H-tetrazolium, sodium salt] (Dojindo Laboratories,

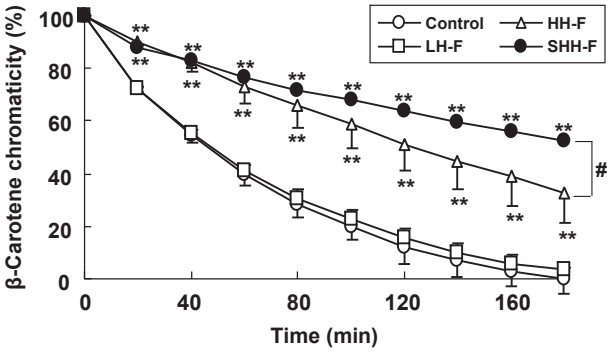

Figure 3. Antioxidative activities of hydroxylated fullerene derivatives against auto-oxidation of linoleic acid/β-Carotene. Antioxidative activity was assessed by a β-Carotene bleaching method. The suppression of discolouration of β-Carotene/linoleic acid aliquots reflects its antioxidative ability. After addition of LH–F, HH-F, SHH-F (60 μM) or water (Control) into the β-Carotene/linoleic acid aliquots, the temporal changes of β-Carotene-attributed chromaticity (percentage of the initial absorbance) was monitored. Values are expressed as mean ± SD ($n = 3$). Significantly different from control, $^{**}p < 0.01$ (vs water); $^{\#}p < 0.05$ (SHH-F vs HH-F).

Kumamoto, Japan) to yellowish formazan, which is indicative of viable cells. After incubation for the indicated days, cells were rinsed with phenol red (PR)-free medium and then incubated for 3 h in PR-free MEM containing 5 mM WST-1 and 0.2 mM 1-methoxy-5-methylphenazinium methylsulphate at 37°C. The absorbance at 450 nm was measured with a microplate reader. The absorption of SHH-F at 450 nm was negligible. In addition, cells were stained with Diff-Quik, photographed for five fields per well (20 fields in total under each condition), counted under a microscope and calculated for the cell number.

Statistical analysis

Data were expressed as mean ± SD and statistical comparisons were performed using an unpaired Student's *t*-test or a Dunnet's multiple comparison test. Differences with $p < 0.05$ or $p < 0.01$ were considered to be statistically significant.

Results

Intracellular ROS production during differentiation of OP9 cells into adipocytes

To investigate the correlation of the differentiation of OP9 cells into adipocytes with intracellular ROS production, we estimated the intracellular ROS level followed by the induction of differentiation. On day 0, OP9 preadipocytes had little intracellular lipids (Figure 2A) and showed a low ROS level (Figure 2B). During the following days, cells rapidly acquired a round hypertrophic shape and accumulated lipid droplets (Figures 2A and B) and progressively increased ROS levels in a specific cytoplasmic area (Figure 2C). Both lipid accumulation and ROS levels in adipocytes are significantly higher than those of preadipocytes (day 0) (Figure 2D). Moreover, differentiation-induced intracellular ROS levels tended to positively correlate with lipid accumulation levels (Figure 2E). These results indicate that increases in lipid accumulation were followed by intracellular ROS generation. Therefore, it is suggested that both adipocyte differentiation and lipid accumulation are closely implicated in generation of ROS.

Antioxidative activity of hydroxylated fullerene derivatives

To evaluate the differences in antioxidative activity among three types of hydroxylated fullerene derivatives (LH-F, HH-F and SHH-F), which bear different numbers of hydroxyl groups, we investigated the suppressive effects of LH-F, HH-F and SHH-F on auto-oxidation of linoleic acid by a β-Carotene bleaching method. The antioxidant activity reflects the retention of β-Carotene-attributed yellowish-orange colour, which disappeared by oxidized linoleic acid. SHH-F and HH-F significantly delayed the time-dependent fading of yellowish colour of β-Carotene as compared with the control, whereas LH-F showed scarcely an antioxidative activity (Figure 3). The residual ratios of SHH-F, HH-F and LH-F were 52.4%, 37.7% and 3.0%, respectively, in comparison with the control (water). Thus, these results showed that SHH-F has a more powerful antioxidative ability than the two other fullerenols.

Suppressive effects of hydroxylated fullerene derivatives on intracellular lipid accumulation in OP9 cells during differentiation

During the differentiation of OP9 preadipocytes into adipocytes, the cells were treated with hydroxylated fullerene derivatives on days 3 and 5 and intracellular oil droplets were stained with Oil Red O and quantified (Figures 4A–C). At the end of the induction of differentiation (day 9), the intracellular lipid accumulation level was increased to 210% as compared with the induction (−). SHH-F and HH-F significantly suppressed lipid accumulation relative to the induction (+) of the control cells in a dose-dependent manner (Figure 4C). However, LF-H scarcely suppressed the lipid accumulation at any concentration. These results exhibited that SHH-F or HH-F exerted a more effective activity for suppression of lipid accumulation than LH-F.

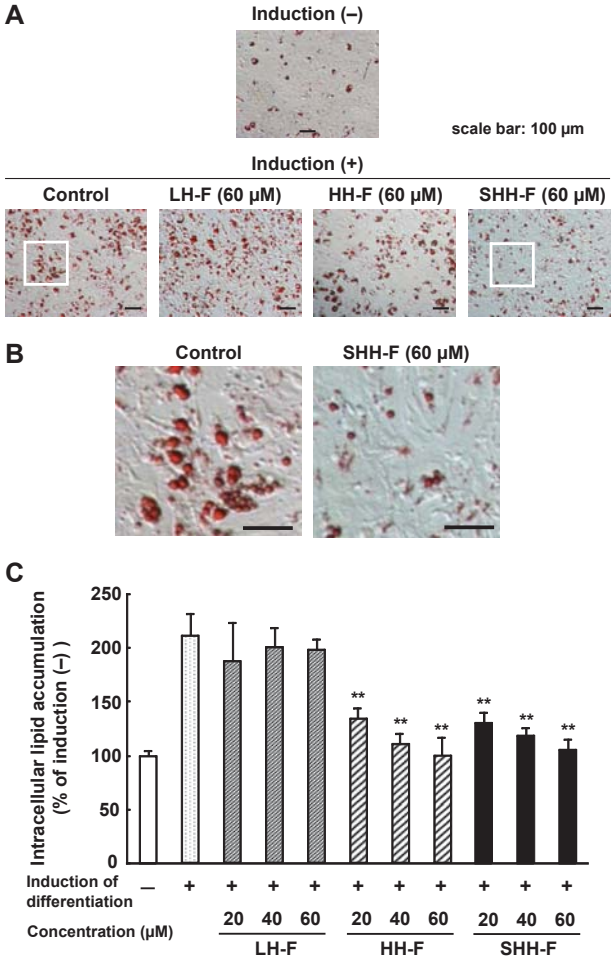

Figure 4. Inhibitory effects of hydroxylated fullerene derivatives on intracellular lipid accumulation in OP9 cells during differentiation. OP9 cells were differentiated into adipocytes as described in Materials and methods. Intracellular lipid accumulation was determined by Oil Red O staining on 7 days after induction of differentiation. Morphological aspects of Oil Red O-stained cells were photographed under a microscope (A) and subsequently the dye was extracted and the absorbance was determined. Areas inside the white boxes in (A) were enlarged and represented in (B). The intracellular lipid accumulation level is expressed as a percentage vs that of the induction (−) cells (C). Concentration values represent C60 equivalent molarity (μM) in each fullerene. The scale bar indicates 100 μm. Values are expressed as mean ± SD (n = 4–8). Significantly different from induction (+), $^{**}p < 0.01$.

Cytotoxicity of SHH-F in OP9 cells

To estimate the cytotoxicity of SHH-F, we evaluated cell viability by two methods: cell viability based on mitochondrial activity and cell number based on cell counting. After treatment with the medium containing varying concentrations of SHH-F for 7 days, the results obtained by two different methods showed similar tendencies that the cell viabilities were decreased in a dose-dependent manner (Figure 5). In particular, the reduction of cell viabilities was significant over 120 μM of SHH-F.

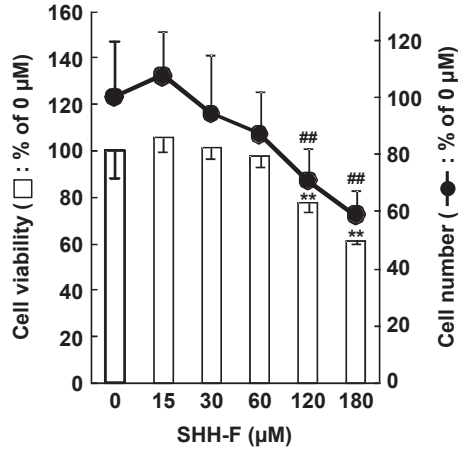

Figure 5. Cytotoxicity of SHH-F in OP9 cells during differentiation. OP9 cells were treated with various concentrations of SHH-F for 7 days during differentiation. Cell viability was determined by WST-1 assay or cell counting on 7 days. Cell viability and cell number was expressed as a percentage of the 0 μM (non-treated cells). Each concentration (μM) indicates fullerene equivalent. Values are expressed as mean ± SD (n = 4). Significantly different from the control: $^{**}p < 0.01$ for cell viability; $^{\#\#}p < 0.01$ for cell number.

Repressive effects of SHH-F on intracellular ROS production during differentiation of OP9 cells into adipocytes

From the result of the cytotoxicity test, we investigated the effects of SHH-F on intracellular lipid accumulation in OP9 cells during differentiation at 0, 30 and 60 μM, since the cell viabilities of OP9 cells were not markedly decreased below the concentration of 60 μM (Figure 5). To correct the even subtle changes in cell numbers in these concentration ranges and evaluate the suppressive effects of SHH-F more accurately, we measured not only the lipid accumulation levels but also the cell number and calculated the intracellular lipid accumulation levels per 10^4 cells (percentage of induction (-)). Furthermore, to examine whether SHH-F could prevent the increase in intracellular ROS accompanied by differentiation, we quantified the intracellular ROS levels by NBT assay. The ROS levels were also expressed as the value per 10^4 cells. Our results showed that intracellular lipids and ROS levels markedly increased after induction of differentiation (Figures 6A–C). The treatment with SHH-F significantly decreased both increases in intracellular lipids and ROS levels in a dose-dependent manner (Figures 6A–D). The repressive effects of SHH-F were attenuated in comparison with the results in Figure 4C. This discrepancy was attributed to the adjustment of the intracellular lipid accumulation levels based on cell number. On the other hand, the positive correlation of intracellular ROS with lipid levels is observed as well as the result of Figure 2 and the slopes were changed into more gentle patterns by SHH-F treatment in a dose-dependent manner (Figure 6E). These findings suggest that SHH-F can

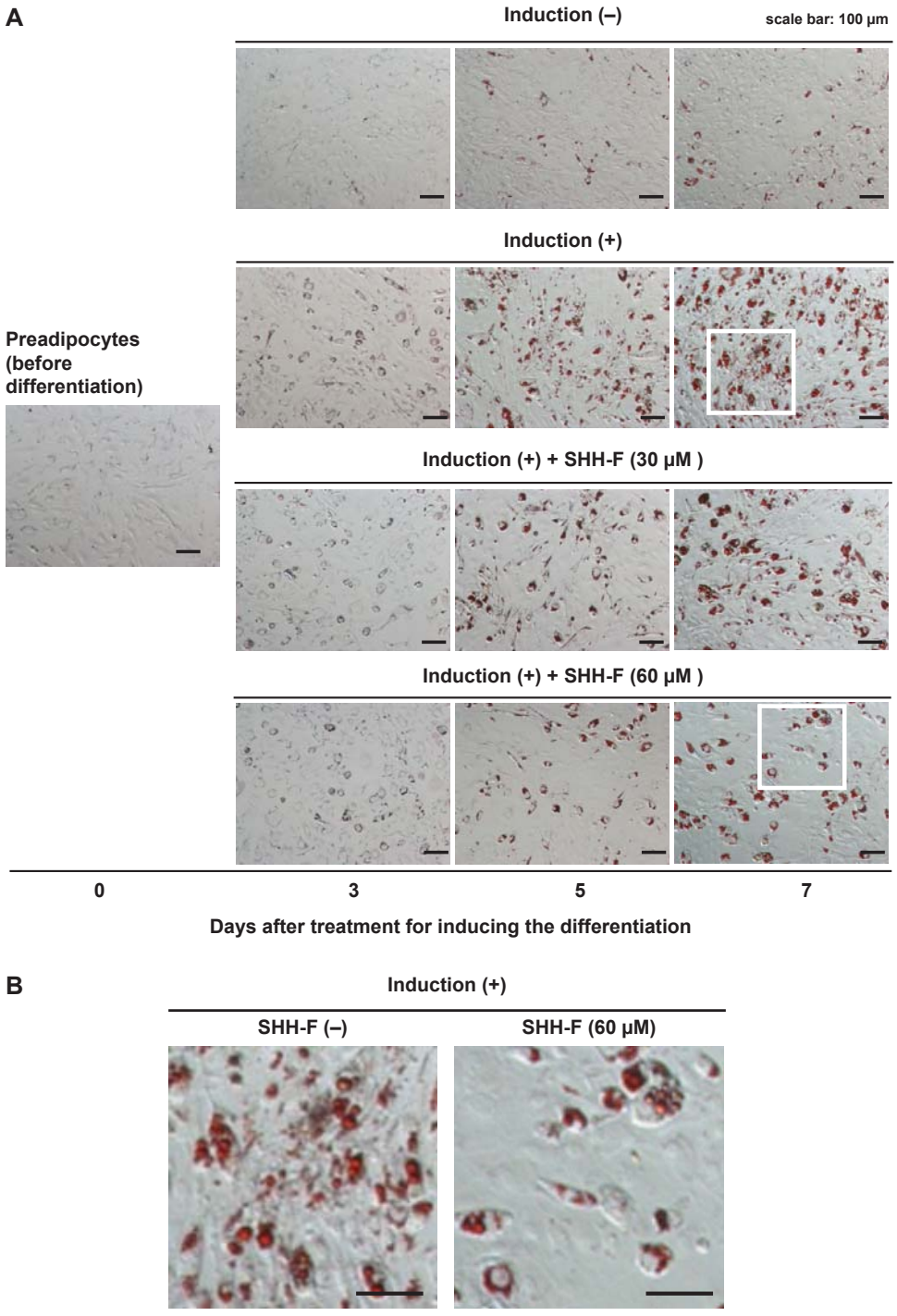

Figure 6. Suppressive effects of SHH-F on intracellular lipid accumulation and ROS generation in OP9 cells during differentiation. OP9 cells were differentiated to adipocytes as described in Materials and methods. Intracellular lipid accumulation and ROS production were determined by Oil Red O staining and NBT reduction on the indicated days, respectively. Morphological aspects of Oil Red O-stained (A) or NBT-stained (C) OP9 cells during differentiation into adipocytes were photographed under a microscope. Subsequently, intracellular lipid accumulation levels were analysed by an Image J software and NBT-derived formazan was extracted and measured for the absorbance (D). Intracellular lipid accumulation levels of the cells without differentiation induction at 7th day were set at 100%. Areas inside the white boxes in (A) were enlarged and represented in (B). Correlation of intracellular ROS with lipid accumulation and Pearson's correlation coefficient (r) are shown for each relationship. Each data point was calculated from the average of independent data ($n = 3$) (E). The scale bar indicates 100 μm. Each concentration (μM) indicates fullerene equivalent. Values are expressed as mean ± SD ($n = 3$). Significantly different from induction (+) at the same day, $^{*}p < 0.05$, $^{**}p < 0.01$ (lipid accumulation); # $p < 0.05$, ## $p < 0.01$ (intracellular ROS).

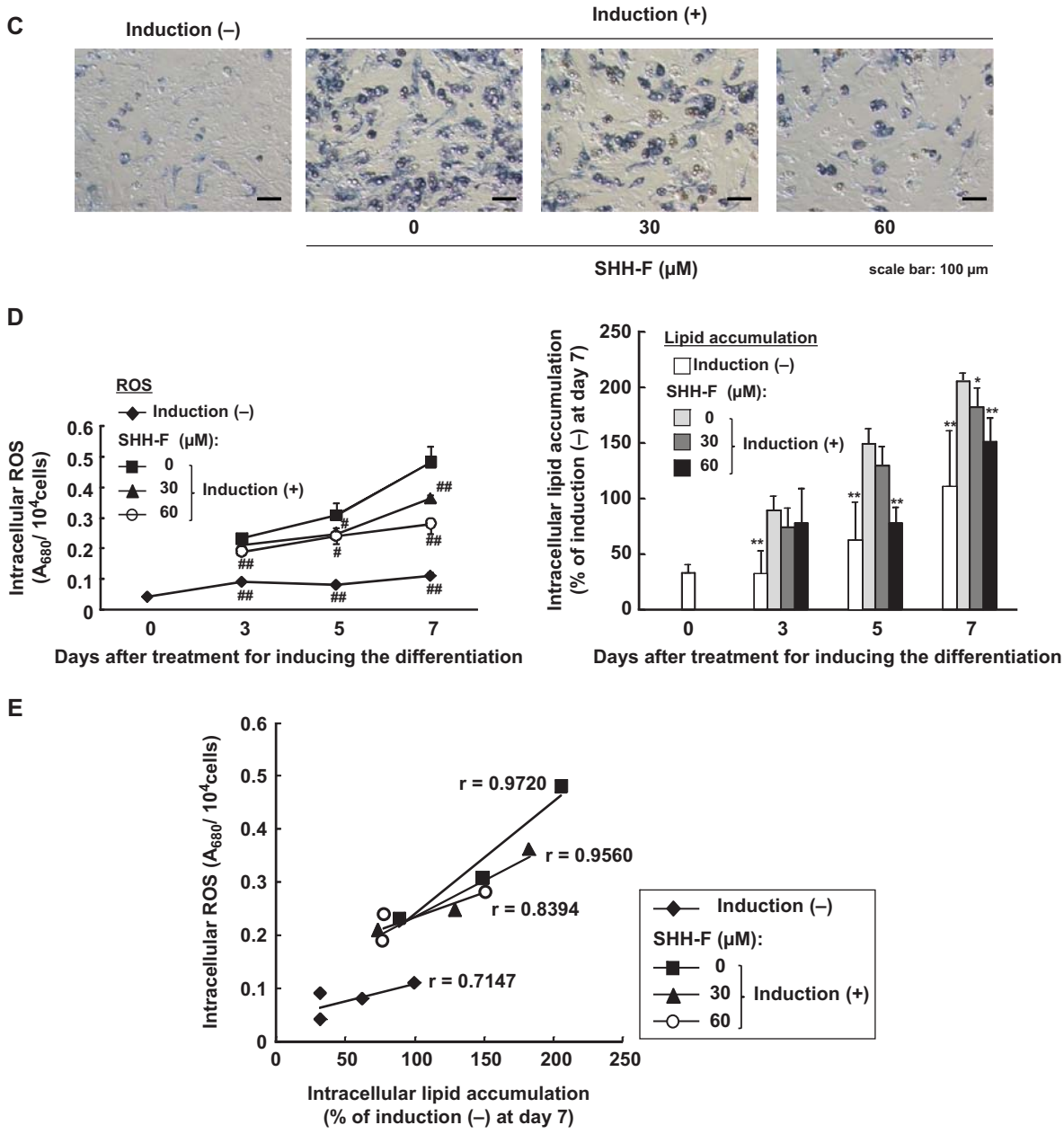

Figure 6. *(Continued)*

suppress intracellular ROS which is generated concurrently with differentiation into adipocytes.

Discussion

In the present study, we investigated the suppressive effects of three types of fullerenols ($C_{60}(OH)_{6-12}$; LH-F, $C_{60}(OH)_{32-34}\cdot 7H_2O$; HH-F and $C_{60}(OH)_{44}\cdot 8H_2O$; SHH-F) on intracellular lipid accumulation and intracellular ROS generation during the differentiation of OP9 preadipocytes into adipocytes. Our results obviously indicated that differentiation from preadipocytes to adipocytes are followed by gradual increases in intracellular lipid accumulation and intracellular ROS generation and the differentiation-dependent augmentation of lipid level was positively correlated with the intracellular ROS level (Figure 2E). Similar results have been observed in 3T3-L1 preadipocytes [20], which is one of the most frequently studied pre-adipocyte cell lines, and in both the liver and adipose tissue of mice fed a high-fat diet [22]. ROS plays essential roles in adipogenesis by transcriptional regulation of adipocyte-specific diverse genes such as adiponectin, peroxisome proliferator-activated receptor-γ (PPARγ), plasminogen activator inhibitor–1 (PAI-1), IL-6 and monocyte chemotactic protein–1 (MCP-1) in 3T3-L1 adipocytes [20]. It has also been demonstrated that the pathways for ROS production and oxidative stress are coordinately up-regulated in both the liver and adipose tissue of mice fed a high-fat diet before the onset of insulin resistance and obesity and the increased ROS production preceded the elevation of tumour necrosis factor-α and free fatty acids in the

plasma and liver [22]. Thus, obesity is an important factor for enhanced oxidative stress and the oxidative stress triggers the development of insulin resistance and inflammatory response [21,29]. These results suggest that the increases in intracellular lipid accumulation in parallel with ROS generation in adipocytes can be a useful therapeutic target for prevention of obesity and obesity-related diseases.

Fullerenol is one of the major water-soluble fullerene derivatives and is found to possess particular significance as a free radical scavenger or an antioxidant in biological systems [1–11]. Our results demonstrated that a novel polyhydroxylated fullerene SHH-F showed the superior antioxidative activity to two other types of hydroxylated fullerene derivatives (LH-F and HH-F) (Figure 3). The inhibitory effects of hydroxylated fullerene derivatives on intracellular lipid accumulation had a tendency to enhance by the number of fullerene hydroxyl groups (Figure 4) and these results indicated that the inhibitory effects of hydroxylated fullerene derivatives on intracellular lipid accumulation were related to the difference of numbers of fullerene hydroxyl groups. A similar tendency was appreciated in the antimicrobial activity [30]. It has known that fullerenols with fewer than 12 hydroxyl groups on fullerene cage show very poor water-solubility [31], whereas fullerenols with more numerous hydroxyl groups exhibit good water-solubility [32]. Therefore, one of the presumed reasons is the increase in bioavailability of fullerenol by enhancement of water-solubility due to the addition of hydroxyl groups.

It has previously been demonstrated that lipophilic antioxidant (±)-α-tocopherol showed an antioxidative activity, but the water-soluble antioxidant ascorbic acid scarcely exerted an antioxidative activity in a β-Carotene bleaching method [7]. Thus, this method can mainly detect an antioxidative potential in the lipophilic region. Our results suggest that the lipophilic antioxidative activity of SHH-F is quite important to suppress ROS generation in lipid-abundant adipocytes (Figure 6). Indeed, we also demonstrated that SHH-F effectively suppressed the differentiation-related changes as compared with LH-F (Figure 4). These results also imply that antioxidants, which possess excellent lipophilic antioxidative potential as well as bioavailability, might be useful tools for prevention of lipid accumulation in adipocytes.

The cytotoxic effects of fullerenols were not neglected from a viewpoint of application as lipid metabolism-improving agents. Although treatment with higher concentrations of SHH-F significantly reduced cell viability (Figure 5), our results demonstrated that the suppressive effects of SHH-F on intracellular lipid accumulation in OP9 cells were found in the range of concentration that scarcely affects the cell viability. It has been reported that fullerenols exhibit cytotoxic effects in some kinds of cell lines [9,14–16,33,34] due to numbers of hydroxyl groups and cytotoxic properties of coexistent impurities. Hence, the higher concentrations of SHH-F that induced a decrease in cell viability might be attributed to its cytotoxicity. On the other hand, it is well-known that obesity is the result of both increased adipocyte size and increased adipocyte number [35]; therefore, inductions of growth arrest and/or apoptosis in adipocytes were noted as a viewpoint of regulation of obesity [36–41]. This concept indicates that the decreases in cell viability at higher concentration of SHH-F might have a suppressive potential against obesity through induction of growth arrest or apoptosis in adipocytes and it might show a different behaviour from lower and non-toxic concentrations. It is not clearly concluded whether the decreases in cell viability at higher concentrations of SHH-F were due to induction of growth arrest or apoptosis or its cytotoxicity in the present study. Therefore, additional investigations are still necessary for utilizing fullerenols for biological applications. In conclusion, our results demonstrate that SHH-F showed a stronger antioxidative activity and more suppressive effects against differentiation-dependent increases in intracellular lipid accumulation and ROS generation during differentiation than two other lower-hydroxylated fullerernols. Therefore, the novel fullerene derivative SHH-F is suggested to be a possible candidate for controlling of obesity and metabolic syndrome and deserves further investigation, including not only biological effects but also its toxicological properties.

Declaration of interest: This work was performed as a part of the Research and Development Project of Industrial Science and Technology Frontier Program supported as a grant-in aid by NEDO (New Energy and Industrial Technology Development Organization), Japan, to N.M.

References

[1] Yin JJ, Lao F, Fu PP, Wamer WG, Zhao Y, Wang PC, Qiu Y, Sun B, Xing G, Dong J, Liang XJ, Chen C. The scavenging of reactive oxygen species and the potential for cell protection by functionalized fullerene materials. Biomaterials 2009;30:611–621.

[2] Yamawaki H, Iwai N. Cytotoxicity of water-soluble fullerene in vascular endothelial cells. Am J Physiol Cell Physiol 2006;290:1495–1502.

[3] Tsai MC, Chen YH, Chiang LY. Polyhydroxylated C60, fullerenol, a novel free-radical trapper, prevented hydrogen peroxide- and cumene hydroperoxide-elicited changes in rat hippocampus *in vitro*. J Pharm Pharmacol 1997;49: 438–445.

[4] Chiang LY, Lu F-J, Lin J-T. Free radical scavenging activity of water-soluble fullerenols. J Chem Soc Chem Commun 1995;12:1283–1284.

[5] Lai HS, Chen Y, Chen WJ, Chang J, Chiang LY. Free radical scavenging activity of fullerenol on grafts after small bowel transplantation in dogs. Transplant Proc 2000;32: 1272–1274.

[6] Lai HS, Chen WJ, Chiang LY. Free radical scavenging activity of fullerenol on the ischemia-reperfusion intestine in dogs. World J Surg 2000;24:450–454.

[7] Kato S, Aoshima H, Saitoh Y, Miwa N. Highly hydroxylated or gamma-cyclodextrin-bicapped water-soluble derivative of

fullerene: the antioxidant ability assessed by electron spin resonance method and beta-carotene bleaching assay. Bioorg Med Chem Lett 2009;19:5293–5296.

[8] Kamat JP, Devasagayam TP, Priyadarsini KI, Mohan H. Reactive oxygen species mediated membrane damage induced by fullerene derivatives and its possible biological implications. Toxicology 2000;155:55–61.

[9] Isakovic A, Markovic Z, Todorovic-Markovic B, Nikolic N, Vranjes-Djuric S, Mirkovic M, Dramicanin M, Harhaji L, Raicevic N, Nikolic Z, Trajkovic V. Distinct cytotoxic mechanisms of pristine versus hydroxylated fullerene. Toxicol Sci 2006;91:173–183.

[10] Dugan LL, Gabrielsen JK, Yu SP, Lin TS, Choi DW. Buckminsterfullerenol free radical scavengers reduce excitotoxic and apoptotic death of cultured cortical neurons. Neurobiol Dis 1996;3:129–135.

[11] Djordjevic A, Bogdanovic G, Dobric S. Fullerenes in biomedicine. J BUON 2006;11:391–404.

[12] Lai YL, Chiang LY. Water-soluble fullerene derivatives attenuate exsanguination-induced bronchoconstriction of guinea-pigs. J Auton Pharmacol 1997;17:229–235.

[13] Jin H, Chen WQ, Tang XW, Chiang LY, Yang CY, Schloss JV, Wu JY. Polyhydroxylated C60, fullerenols, as glutamate receptor antagonists and neuroprotective agents. J Neurosci Res 2000;62:600–607.

[14] Chen YW, Hwang KC, Yen CC, Lai YL. Fullerene derivatives protect against oxidative stress in RAW 264.7 cells and ischemia-reperfused lungs. Am J Physiol Regul Integr Comp Physiol 2004;287:21–26.

[15] Bogdanovic G, Kojic V, Dordevic A, Canadanovic-Brunet J, Vojinovic-Miloradov M, Baltic VV. Modulating activity of fullerol C60(OH)22 on doxorubicin-induced cytotoxicity. Toxicol *In Vitro* 2004;18:629–637.

[16] Lu LH, Lee YT, Chen HW, Chiang LY, Huang HC. The possible mechanisms of the antiproliferative effect of fullerenol, polyhydroxylated C60, on vascular smooth muscle cells. Br J Pharmacol 1998;123:1097–1102.

[17] Roursgaard M, Poulsen SS, Kepley CL, Hammer M, Nielsen GD, Larsen ST. Polyhydroxylated C60 fullerene (fullerenol) attenuates neutrophilic lung inflammation in mice. Basic Clin Pharmacol Toxicol 2008;103:386–388.

[18] Cai X, Jia H, Liu Z, Hou B, Luo C, Feng Z, Li W, Liu J. Polyhydroxylated fullerene derivative C(60)(OH)(24) prevents mitochondrial dysfunction and oxidative damage in an MPP(+) -induced cellular model of Parkinson's disease. J Neurosci Res 2008;86:3622–3634.

[19] Kopelman PG. Obesity as a medical problem. Nature-. 2000;404:635–643.

[20] Furukawa S, Fujita T, Shimabukuro M, Iwaki M, Yamada Y, Nakajima Y, Nakayama O, Makishima M, Matsuda M, Shimomura I. Increased oxidative stress in obesity and its impact on metabolic syndrome. J Clin Invest. 2004;114:1752-1761.

[21] Urakawa H, Katsuki A, Sumida Y, Gabazza EC, Murashima S, Morioka K, Maruyama N, Kitagawa N, Tanaka T, Hori Y, Nakatani K, Yano Y, Adachi. Oxidative stress is associated with adiposity and insulin resistance in men. J Clin Endocrinol Metab 2003;88:4673–4676.

[22] Matsuzawa-Nagata N, Takamura T, Ando H, Nakamura S, Kurita S, Misu H, Ota T, Yokoyama M, Honda M, Miyamoto K, Kaneko S. Increased oxidative stress precedes the onset of high-fat diet-induced insulin resistance and obesity. Metabolism 2008;57:1071–1077.

[23] Diniz YS, Rocha KK, Souza GA, Galhardi CM, Ebaid GM, Rodrigues HG, Novelli Filho JL, Cicogna AC, Novelli EL. Effects of N-acetylcysteine on sucrose-rich diet-induced hyperglycaemia, dyslipidemia and oxidative stress in rats. Eur J Pharmacol 2006;543:151–157.

[24] Wolins NE, Quaynor BK, Skinner JR, Tzekov A, Park C, Choi K, Bickel PE. OP9 mouse stromal cells rapidly differentiate into adipocytes: characterization of a useful new model of adipogenesis. J Lipid Res 2006;47:450–460.

[25] Kokubo K, Matsubayashi K, Tategaki H, Takada H, Oshima T. Facile synthesis of highly water-soluble fullerenes more than half-covered by hydroxyl groups. ACS Nano 2008;2: 327–333.

[26] Ramirez-Zacarias JL, Castro-Munozledo F, Kuri-Harcuch W. Quantitation of adipose conversion and triglycerides by staining intracytoplasmic lipids with Oil red O. Histochemistry 1992;97:493–497.

[27] Schrenzel J, Serrander L, Bánfi B, Nüsse O, Fouyouzi R, Lew DP, Demaurex N, Krause. Electron currents generated by the human phagocyte NADPH oxidase. Nature 1998;392: 734–737.

[28] Emmons C, Peterson DM. Antioxidant activity and phenolic contents of oat groats and hulls. Cereal Chemistry 1999;76: 902–906.

[29] Lin Y, Berg AH, Iyengar P, Lam TK, Giacca A, Combs TP, et al. The hyperglycemia-induced inflammatory response in adipocytes: the role of reactive oxygen species. J Biol Chem 2005;280:4617–4626.

[30] Aoshima H, Kokubo K, Shirakawa S, Ito M, Yamana S, Oshima T. Antimicrobial activity of fullerenes and their hydroxylated derivatives. Biocontrol Sci 2009;14:69–72.

[31] Chiang LY, Wang LY, Swirczewski JW, Soled S, Cameron S. Efficient synthesis of polyhydroxylated fullerene derivatives via hydrolysis of polycyclosulfated precursors. J Org Chem 1994;59:3960–3968.

[32] Wang S, He P, Zhang J-M, Jiang H, Zhu S-Z. Novel and efficient synthesis of water-soluble [60] fullerenol by solvent-free reaction. Synth Commun 2005;35:1803–1807.

[33] Sayes C, Fortner JD, Guo W, Lyon D, Boyd AM, Ausman KD, Tao YJ, Sitharaman B, Wilson LJ, Hughes J, West JL, Colvin VL. The differential cytotoxicity of water-soluble fullerenes. Nano Letters 2004;4:1881–1887.

[34] Sayes CM, Gobin AM, Ausman KD, Mendez J, West JL, Colvin VL. Nano-C60 cytotoxicity is due to lipid peroxidation. Biomaterials 2005;26:7587–7595.

[35] Wolfram S, Wang Y, Thielecke F. Anti-obesity effects of green tea: from bedside to bench. Mol Nutr Food Res 2006;50:176–187.

[36] Moon HS, Chung CS, Lee HG, Kim TG, Choi YJ, Cho CS. Inhibitory effect of (-)-epigallocatechin-3-gallate on lipid accumulation of 3T3-L1 cells. Obesity (Silver Spring) 2007; 15:2571–2582.

[37] Morikawa K, Ikeda C, Nonaka M, Pei S, Mochizuki M, Mori A, Yamada S. Epigallocatechin gallate-induced apoptosis does not affect adipocyte conversion of preadipocytes. Cell Biol Int 2007;31:1379–1387.

[38] Morikawa K, Nonaka M, Mochizuki H, Handa K, Hanada H, Hirota K. Naringenin and hesperetin induce growth arrest, apoptosis, and cytoplasmic fat deposit in human preadipocytes. J Agric Food Chem 2008;56:11030–11037.

[39] Yang JY, Della-Fera MA, Rayalam S, Ambati S, Hartzell DL, Park HJ, Baile CA. Enhanced inhibition of adipogenesis and induction of apoptosis in 3T3-L1 adipocytes with combinations of resveratrol and quercetin. Life Sci 2008;82: 1032–1039.

[40] Rayalam S, Yang JY, Ambati S, Della-Fera MA, Baile CA. Resveratrol induces apoptosis and inhibits adipogenesis in 3T3-L1 adipocytes. Phytother Res 2008;22:1367–1371.

[41] Xiao Y, Yuan T, Yao W, Liao K. 3T3-L1 adipocyte apoptosis induced by thiazolidinediones is peroxisome proliferator-activated receptor-gamma-dependent and mediated by the caspase-3-dependent apoptotic pathway. FEBS J 2010;277: 687–696.

This paper was first published online on Early online on 2 July 2010.